EVANICHITE, Pb$_6$Cr^{3+}(Cr^{6+}O$_4$)$_2$(SO$_4$)(OH)$_7$FCl, FROM TIGER, ARIZONA, USA, THE FIRST MINERAL CONTAINING BOTH Cr^{3+} AND Cr^{6+}

Hexiong YANG[§], Ronald B. GIBBS, Francis X. SOUSA, and Robert T. DOWNS

Department of Geosciences, University of Arizona, 1040 E. 4th Street, Tucson, Arizona 85721-0077, USA

ABSTRACT

A new mineral species, evanichite (IMA 2022-033), ideally Pb$_6$Cr^{3+}(Cr^{6+}O$_4$)$_2$(SO$_4$)(OH)$_7$FCl, has been discovered from the Mammoth-Saint Anthony mine, Tiger, Arizona, USA. It occurs as a single group of subparallel short prismatic crystals on top of a quartz matrix. Individual crystals are up to $0.70 \times 0.20 \times 0.20$ mm in size. Associated minerals include georgerobinsonite, bobmeyerite, pinalite, diaboleite, boleite, leadhillite, caledonite, cerussite, calcite, baryte, and fluorite. Evanichite is orange-brown to red-brown in transmitted light, transparent with a white streak and an adamantine luster. It is brittle and has a Mohs hardness of 2½–3 with perfect cleavage on {100}. No twinning was observed. The calculated density is 5.878 g/cm^3. Evanichite is insoluble in water or hydrochloric acid. An electron probe microanalysis yielded an empirical formula [based on 21 (O+F+Cl) *apfu*] of Pb$_{5.91}$(Cr$^{3+}_{0.81}$Fe$^{3+}_{0.11}$)$_{\Sigma0.92}$(Cr^{6+}O$_4$)$_2$(S$_{1.07}$O$_4$)(OH)$_7$F$_{0.99}$Cl$_{1.05}$, which can be simplified to Pb$_6$(Cr^{3+}, Fe^{3+})(Cr^{6+}O$_4$)$_2$(SO$_4$)(OH)$_7$FCl.

Evanichite is trigonal with space group $P3$ and unit-cell parameters $a = 7.7651(14)$, $c = 9.6199(17)$ Å, $V = 502.3(2)$ Å^3, and $Z = 1$. Its crystal structure consists of two unique Pb polyhedra [Pb1 coordinated by (5O + 3OH) and Pb2 by (5O + 2OH + F + Cl)], one M^{3+}(OH)$_6$ octahedron ($M = $ Cr^{3+} + Fe^{3+}), two Cr^{6+}O$_4$ tetrahedra (Cr1 and Cr2), and one SO$_4$ tetrahedron. These polyhedra form four different layers parallel to (001). Layer 1 consists of edge- and corner-shared Pb1 polyhedra, layer 2 of isolated Cr1 and Cr2 tetrahedra, layer 3 of edge- and corner-shared Pb2 polyhedra, and layer 4 of isolated Cr^{3+}(OH)$_6$ octahedra and SO$_4$ tetrahedra. These layers are stacked along [001] in the sequence layer 4 + layer 3 + layer 2 + layer 1 + layer 4. Both Pb1 and Pb2 cations are coordinated to anions with four short Pb–Φ ($\Phi = $ O, OH, F, or Cl) distances between 2.37 and 2.60 Å on one side and four (for Pb1) or five (for Pb2) long Pb–Φ distances ranging from 2.84 and 3.19 Å on the other side, indicating that both of them are lone-pair stereoactive. Evanichite is the first mineral that contains both Cr^{3+} and Cr^{6+}, as well as the first chromate-sulfate compound with (CrO$_4$)$^{2-}$ and (SO$_4$)$^{2-}$ occupying distinct crystallographic sites.

Keywords: evanichite, Pb chromate, new mineral, crystal structure, X-ray diffraction, Raman spectra, Tiger.

INTRODUCTION

A new mineral species, evanichite, ideally Pb$_6$Cr^{3+}(Cr^{6+}O$_4$)$_2$(SO$_4$)(OH)$_7$FCl, was found from the Mammoth-Saint Anthony mine, Tiger, Arizona, USA. It is named in honor of Mr. Daniel J. Evanich (b. 1951), a long-time field collector of Western U.S. minerals and a self-taught amateur mineralogist. Mr. Evanich earned a B.S. degree in Business Administration and retired after a successful career spanning 24 years with the Sony and Panasonic Corporations. He has been a mineral collector for more than three decades with a special interest in mining history and minerals from Butte, Montana, and Tiger, Arizona. Mr. Evanich is an active member of Bay Area Mineralogists of Northern California and has served as a field-trip coordinator for more than 10 years. He is also an active member of both Mineralogical Society of Southern California and Northern California Mineralogical Association. In the past few years, Mr. Evanich has kindly and generously donated or provided a number of mineral samples to the RRUFF Project (http://rruff.info) for data collections and research, including the evanichite specimen, which was obtained by him from the recycled collection of J.F. McCown Jr. in 2017, who had previously obtained it from R.W. (Dick) Thomssen. The new mineral and its name have been approved by the Commission on New Minerals, Nomenclature and Classification (CNMNC) of the International Mineralogical Associ-

§ *Corresponding author e-mail address*: hyang@arizona.edu

FIG. 1. The specimen on which the new mineral evanichite, indicated by the green arrow, was found.

FIG. 2. A microscopic view of brown crystals of evanichite on top of the quartz matrix. The blue mineral is diaboleite.

ation (IMA 2022-033). The co-type samples have been deposited at the University of Arizona Alfie Norville Gem and Mineral Museum (Catalogue # 22718) and the RRUFF Project (deposition # R220006) (http://rruff. info). This paper describes the physical and chemical properties of evanichite, and its crystal structure determined from single-crystal X-ray diffraction data[1].

SAMPLE DESCRIPTION AND EXPERIMENTAL METHODS

Occurrence, physical and chemical properties, and Raman spectra

Evanichite was found on a specimen (Fig. 1) collected from the Mammoth-Saint Anthony mine ($32°42'23''$N, $110°40'59''$W), Tiger, Pinal County, Arizona, USA. The host matrix for evanichite is quartz, and associated minerals include georgerobinsonite, bobmeyerite, pinalite, diaboleite, boleite, leadhillite, caledonite, cerussite, calcite, baryte, and fluorite. In addition to evanichite, described herein, the Mammoth-St. Anthony mine is also the type locality for ten other minerals, including bideauxite $AgPb_2F_2Cl_3$, bobmeyerite $Pb_4(Al_3Cu)(Si_4O_{12})(S_{0.5}Si_{0.5}O_4)(OH)_7Cl(H_2O)_3$, creaseyite $Cu_2Pb_2Fe^{3+}_2Si_5O_{17}\cdot6H_2O$, georgerobinsonite $Pb_4(CrO_4)_2(OH)_2FCl$, macquartite $Cu_2Pb_7(CrO_4)_4(SiO_4)_2(OH)_2$, mammothite $Pb_6Cu_4AlSb^{5+}O_2(SO_4)_2Cl_4(OH)_{16}$, murdochite Cu_{12} $Pb_2O_{15}Cl_2$, pinalite $Pb_3(WO_4)OCl_2$, wherryite $Pb_7Cu_2(SO_4)_4(SiO_4)_2(OH)_2$, and yedlinite $Pb_6Cr(Cl,OH)_6(OH,O)_8$.

Mineralization in the Mammoth-St. Anthony mine is a series of veins within shear zones that strike WNW and dip steeply SW. Their gangue consists of brecciated country rock cemented and replaced with quartz and calcite together with some baryte and fluorite. The quartz forms successive bands of which some of the latest generation show well-developed comb structure and are locally amethystine. Wall rock alteration along the veins consists mainly of chloritization and silicification. Such alteration, together with the texture and mineralogy of the veins, points to deposition in the epithermal zone. Detailed descriptions of the mineralogy and geology of the Mammoth-St. Anthony mine, as well as other mineral deposits in Tiger, Arizona, have been given by Bideaux (1980) and Panczner (1982).

Evanichite occurs as a single group of subparallel short prismatic crystals on top of the quartz matrix (Fig. 2). Individual crystals are up to $0.70 \times 0.20 \times 0.20$ mm in size. Evanichite is orange-brown to redbrown in transmitted light, transparent with white streak and adamantine luster. It is brittle and has a Mohs hardness of 2½–3 with perfect cleavage on {100}. No twinning was observed. The density was undetermined because it is greater than available density liquids and there is insufficient material for the direct measurement. The calculated density is 5.878 g/cm³. No optical properties were measured because the indices of refraction are too high for a measurement in our laboratory; no index liquids with n > 2 were available. The calculated average index of refraction is 2.024 for the empirical formula based on the Gladstone-Dale relationship (Mandarino 1981). Evanichite is insoluble in water or hydrochloric acid.

---

[1] Supplementary Data are available from the Depository of Unpublished Data on the MAC website (http://mineralogicalassociation.ca/), document ''Evanichite, CM61, 22-00068''.

TABLE 1. ANALYTICAL DATA (IN wt.%) FOR EVANICHITE

Constituent	Mean	Range	Stand. Dev.	Probe Standard
PbO	74.02	73.03–74.44	0.54	NBS_K0229
Fe_2O_3	0.47	0.29–0.87	0.15	fayalite
Cr_2O_3	12.01	11.45–12.73	0.39	chromite
Cr_2O_3[*1]	3.47			
CrO_3[*1]	11.24			
SO_3	4.79	4.06–5.14	0.35	baryte
F	1.06	0.80–1.27	0.16	MgF_2
Cl	2.08	1.88–2.25	0.12	Marialite (USNM R6600-1)
O≡F,Cl	−0.92			
H_2O[*2]	3.54			Added in ideal value
Total	99.75	99.52–101.74	0.55	

[*1]: Obtained by adjusting $Cr^{6+} = 2$ *apfu* based on the structure determination (see the structure description below).
[*2]: Assuming 7(OH) *pfu*, based on the structure determination.

The chemical composition of evanichite was determined using a Cameca SX-100 electron microprobe (WDS mode, 15 kV, 20 nA, and a beam diameter of <1 μm). The standards used for the probe analysis are given in Table 1, along with the determined compositions (15 analysis points). The resultant chemical formula, calculated on the basis of 21 O *apfu*, is $Pb_{5.91}(Cr^{3+}_{0.81}Fe^{3+}_{0.11})_{\Sigma 0.92}(Cr^{6+}O_4)_2(S_{1.07}O_4)(OH)_7F_{0.99}Cl_{1.05}$, which can be simplified to $Pb_6(Cr^{3+},Fe^{3+})(Cr^{6+}O_4)_2(SO_4)(OH)_7FCl$.

The Raman spectrum of evanichite (Fig. 3) was collected on a randomly oriented crystal with a Thermo Almega microRaman system using a solid-state laser with a wavelength of 532 nm at the full power of 150 mW and a thermoelectric cooled CCD detector. The laser is partially polarized with 4 cm^{-1} resolution and a spot size of 1 μm.

X-ray crystallography

Both the powder and single-crystal X-ray diffraction data for evanichite were collected on a Bruker X8 APEX2 CCD X-ray diffractometer equipped with graphite-monochromatized Mo$K\alpha$ radiation. Listed in Table 2 (deposited) are the measured powder X-ray diffraction data, along with those calculated from the determined structure using the program XPOW (Downs *et al*. 1993). The unit-cell parameters obtained from the powder X-ray diffraction data are $a = 7.7629(11)$, $c = 9.6246(21)$ Å, and $V = 502.30(13)$ Å^3.

Single-crystal X-ray diffraction data for evanichite were collected from a nearly equidimensional crystal ($0.04 \times 0.03 \times 0.03$ mm) with frame widths of $0.5°$ in ω and 30 s counting time per frame. All reflections were indexed on the basis of a trigonal unit-cell (Table 3).
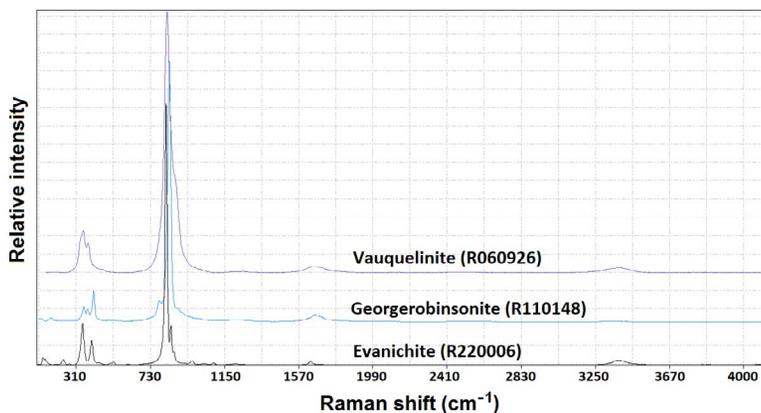

FIG. 3. Raman spectra of evanichite, vauquelinite, and georgerobinsonite.

THE CANADIAN JOURNAL OF MINERALOGY AND PETROLOGY

TABLE 2. POWDER X-RAY DIFFRACTION DATA FOR EVANICHITE

I%	d_{obs}	d_{calc}	h	k	l
10	6.705	6.723	1	0	0
5	5.486	5.511	1	0	1
30	**4.805**	**4.812**	**0**	**0**	**2**
11	3.905	3.913	0	1	2
			1	0	2
100	**3.599**	**3.600**	**1**	**1**	**1**
			2	$\bar{1}$	1
5	3.361	3.361	2	0	0
5	3.208	3.208	0	0	3
			1	1	2
45	**3.023**	**3.021**	**2**	**$\bar{1}$**	**2**
3	2.891	2.895	1	0	3
6	2.755	2.756	0	2	2
42	**2.473**	**2.473**	**1**	**1**	**3**
			2	$\bar{1}$	3
6	2.407	2.406	0	0	4
28	**2.245**	**2.241**	**3**	**0**	**0**
17	2.045	2.045	1	1	4
			2	$\bar{1}$	4
18	2.033	2.032	0	3	2
			3	0	2
6	1.991	1.992	$\bar{1}$	3	3
			1	2	3
			3	$\bar{1}$	3
			2	1	3
4	1.925	1.925	0	0	5
12	1.903	1.902	4	$\bar{2}$	1
			2	2	1
2	1.865	1.865	1	3	0
5	1.837	1.837	0	3	3
5	1.800	1.800	3	0	3
			4	$\bar{2}$	2
			2	2	2
4	1.747	1.747	$\bar{1}$	3	4
5	1.741	1.739	4	$\bar{1}$	2
8	1.725	1.725	1	1	5
4	1.682	1.681	4	0	0
5	1.661	1.661	4	$\bar{2}$	3
			2	2	3
7	1.640	1.640	0	3	4
			3	0	4
2	1.610	1.612	1	3	3
			3	1	3
3	1.587	1.587	0	4	2
			4	0	2
3	1.535	1.534	1	2	5
			2	1	5
4	1.523	1.523	$\bar{3}$	$\bar{2}$	1
2	1.509	1.511	2	2	4
7	1.483	1.482	2	$\bar{1}$	6
6	1.474	1.474	4	$\bar{1}$	4
7	1.461	1.460	3	0	5

TABLE 3. MINERALOGICAL AND STRUCTURE REFINEMENT STATISTICS DATA FOR EVANICHITE

Ideal chemical formula	$Pb_6Cr^{3+}(Cr^{6+}O_4)_2$ $(SO_4)(OH)_7FCl$
Crystal symmetry	Trigonal
Space group	$P3$ (#143)
a (Å)	7.7651(14)
b (Å)	7.7651(14)
c (Å)	9.6199(17)
V (Å^3)	502.34(16)
Z	1
ρ_{cal} (g/cm^3)	5.878
2θ range for data collection	≤ 66.06
No. of reflections collected	4886
No. of independent reflections	2015
No. of reflections with $I > 2\sigma(I)$	1818
No. of parameters refined	95
R(int)	0.0325
Final R_1, wR_2 factors [$I > 2\sigma(I)$]	0.024, 0.044
Goodness-of-fit	0.969

The intensity data were corrected for X-ray absorption using the Bruker program SADABS. The systematic absences of reflections suggest the possible space groups $P3$ or $P\bar{3}$. The crystal structure was solved and refined using SHELX2018 (Sheldrick 2015a, b) based on space group $P3$ because it produced the better refinement statistics in terms of bond lengths and angles, atomic displacement parameters, and R factors. As the X-ray structure analysis is insufficient in distinguishing Cr from Fe due to their similar X-ray scattering powers, their ratio at the octahedrally coordinated M ($= Cr^{3+} + Fe^{3+}$) site was fixed to the normalized value of 0.88/0.12 determined from the electron probe microanalysis. No H atoms were located by the difference Fourier syntheses. All atoms were refined anisotropically. The refinement statistics are listed in Table 3. Final atomic coordinates and displacement parameters are given in Tables 4 and 5, respectively. Selected bond distances are presented in Table 6.

RESULTS AND DISCUSSION

Crystal structure

Evanichite is the first mineral that contains both Cr^{3+} and Cr^{6+}. Its crystal structure contains two unique Pb polyhedra [8-coordinated Pb1 by (5O + 3OH) and 9-coordinated Pb2 by (5O + 2OH + F + Cl)] (Fig. 4), one $M^{3+}(OH)_6$ octahedron, two $Cr^{6+}O_4$ tetrahedra (Cr1 and Cr2), and one SO$_4$ tetrahedron. These polyhedra form four different layers parallel to (001). Layer 1 consists of edge- and corner-shared Pb1 polyhedra

TABLE 4. FRACTIONAL ATOMIC COORDINATES AND EQUIVALENT ISOTROPIC
DISPLACEMENT PARAMETERS ($Å^2$) FOR EVANICHITE

Atom	x	y	z	U_{eq}
Pb1	0.65678 (10)	0.04043 (8)	0.94629 (3)	0.01361 (13)
Pb2	−0.03880 (8)	0.32162 (10)	0.49937 (4)	0.01314 (13)
M*	2/3	1/3	0.2291 (6)	0.0062 (4)
Cr1	1/3	2/3	0.7279 (5)	0.0101 (8)
Cr2	0	0	0.7343 (5)	0.0106 (9)
S	1/3	2/3	0.2119 (4)	0.0088 (8)
O1	1/3	2/3	0.556 (2)	0.017 (4)
O2	0.3667 (16)	0.8851 (14)	0.7854 (12)	0.015 (2)
O3	0	0	0.9044 (18)	0.017 (4)
O4	0.8190 (16)	0.0324 (17)	0.6789 (12)	0.019 (2)
O5	1/3	2/3	0.0573 (17)	0.020 (4)
O6	0.2120 (11)	0.4596 (10)	0.2608 (8)	0.0147 (16)
O7	−0.1304 (15)	0.3372 (15)	0.1012 (12)	0.012 (2)
O8	−0.3288 (15)	0.1354 (14)	0.3590 (11)	0.011 (2)
O9	2/3	1/3	0.8627 (19)	0.011 (3)
F	2/3	1/3	0.5989 (16)	0.016 (3)
Cl	0	0	0.3549 (7)	0.0188 (12)

* M = (0.88Cr + 0.12 Fe).

(Fig. 5a), layer 2 of isolated Cr1 and Cr2 tetrahedra, layer 3 of edge- and corner-shared Pb2 polyhedra (Fig. 5b), and layer 4 of isolated $Cr^{3+}(OH)_6$ octahedra and SO_4 tetrahedra. These layers are stacked along [001] in the sequence layer 4 + layer 3 + layer 2 + layer 1 + layer 4 + ... (Fig. 6). Similar structures consisting of Pb-polyhedral layers alternating with XO_4 (X = Cr^{6+}, S^{6+}, Si^{4+}, As^{5+}, V^{5+}) tetrahedral layers have been observed in many Pb minerals, such as iranite (Yang *et al*. 2007), hemihedrite (Lafuente *et al*. 2017 and

references therein), and georgerobinsonite (Cooper *et al*. 2011).

As illustrated in Figure 4, both Pb1 and Pb2 cations are coordinated to anions with four short Pb–Φ (Φ = O, OH, F, or Cl) distances between 2.37 and 2.60 Å on one side and four (for Pb1) or five (for Pb2) long Pb–Φ distances ranging from 2.84 and 3.19 Å on the other side. Such asymmetric coordination of Pb^{2+} indicates that both Pb1 and Pb2 are lone-pair stereoactive. Details of such behavior of Pb^{2+} cations in a wide range of compounds have been reviewed by Shimoni-

TABLE 5. ATOMIC DISPLACEMENT PARAMETERS ($Å^2$) FOR EVANICHITE

Atom	U^{11}	U^{22}	U^{33}	U^{12}	U^{13}	U^{23}
Pb1	0.0146 (3)	0.0143 (3)	0.0141 (3)	0.0089 (2)	−0.0012 (2)	−0.0029 (2)
Pb2	0.0115 (3)	0.0135 (3)	0.0138 (3)	0.0058 (2)	−0.0024 (2)	0.0005 (2)
M	0.0067 (6)	0.0067 (6)	0.0052 (10)	0.0033 (3)	0	0
Cr1	0.0113 (12)	0.0113 (12)	0.0076 (19)	0.0056 (6)	0	0
Cr2	0.0097 (12)	0.0097 (12)	0.012 (2)	0.0048 (6)	0	0
S	0.0081 (12)	0.0081 (12)	0.010 (2)	0.0040 (6)	0	0
O1	0.012 (5)	0.012 (5)	0.028 (12)	0.006 (3)	0	0
O2	0.016 (5)	0.008 (4)	0.017 (6)	0.004 (4)	−0.002 (4)	−0.003 (4)
O3	0.024 (6)	0.024 (6)	0.004 (9)	0.012 (3)	0	0
O4	0.014 (5)	0.019 (5)	0.021 (6)	0.006 (4)	0.002 (4)	0.006 (5)
O5	0.024 (6)	0.024 (6)	0.012 (9)	0.012 (3)	0	0
O6	0.012 (4)	0.006 (3)	0.020 (4)	0.000 (3)	−0.006 (3)	0.000 (3)
O7	0.009 (5)	0.013 (5)	0.010 (6)	0.003 (4)	0.002 (4)	−0.002 (4)
O8	0.012 (5)	0.013 (5)	0.009 (6)	0.007 (4)	−0.004 (4)	−0.002 (4)
O9	0.013 (5)	0.013 (5)	0.007 (9)	0.007 (2)	0	0
F	0.019 (5)	0.019 (5)	0.010 (8)	0.009 (2)	0	0
Cl	0.0153 (15)	0.0153 (15)	0.026 (4)	0.0076 (8)	0	0

TABLE 6. SELECTED BOND DISTANCES (Å) FOR EVANICHITE

Pb1–O9	2.377(6)	Pb2–O8	2.393(10)
Pb1–O7	2.428(11)	Pb2–F	2.523(6)
Pb1–O2	2.491(11)	Pb2–O8′	2.530(11)
Pb1–O7′	2.541(11)	Pb2–O4	2.601(11)
Pb1–O3	2.864(3)	Pb2–O1	2.843(4)
Pb1–O4	2.879(11)	Pb2–O6	2.850(8)
Pb1–O5	2.930(6)	Pb2–Cl	3.002(3)
Pb1–O2′	3.186(11)	Pb2–O2	3.010(11)
<Pb–O>	2.712	Pb2–O4′	3.185(12)
		<Pb–O>	2.771
Cr1–O1	1.65(2)	Cr2–O1	1.636(18)
Cr1–O2 ×3	1.677(10)	Cr2–O1 ×3	1.636(11)
<Cr1–O>	1.670	<Cr2–O>	1.636
TAV	0.04	TAV	0.23
TQE	1.000	TQE	1.000
M–O7 ×3	1.987(10)	S–O5	1.487(16)
M–O8 ×3	1.995(11)	S–O6 ×3	1.476(7)
<M–O>	1.991	<S–O>	1.479
OAV	24.02	TAV	0.94
OQE	1.006	TQE	1.000

* M = (Cr^{3+} + Fe^{3+}). TAV = tetrahedral angle variance, TQE = tetrahedral quadratic elongation, OAV = Octahedral angle variance, OQE = octahedral quadratic elongation (Robinson *et al.* 1971).

Livny *et al.* (1998). In contrast, all $M^{3+}(OH)_6$ octahedra, $Cr^{6+}O_4$ tetrahedra, and SO_4 tetrahedra are quite regular in terms of average bond distances and polyhedral distortion indices (Robinson *et al.* 1971) (Table 6). For the octahedral M site, despite the substitution of 12% Cr^{3+} by Fe^{3+}, the average <M–O> bond distance (1.991 Å) is still comparable to the average <Cr–O> distances in other Cr^{3+}-bearing minerals, such as 1.991 Å in magnesiochromite ($MgCr_2O_4$) (O'Neill & Dollase 1994) and 1.993 Å kosmochlor $NaCr^{3+}Si_2O_6$ (Origlieri *et al.* 2003).

Although our structure determination was unable to locate H atoms in evanichite, the bond-valence sums, calculated using the parameters given by Brese & O'Keeffe (1991) (Table 7), indicate that O7, O8, and O9 are OH groups. An inspection of the environments around these three OH groups reveals the possible H-bonding schemes: O7–H⋯O6 = 2.793 Å, O8–H⋯F = 2.782 Å, and O9–H⋯O7 = 2.757 Å. The participation of O6 and F in the H-bonds as the acceptors accounts for their noticeably low bond-valence sums, 1.627 v.u. for O6 and 0.792 v.u. for F (Table 7).

Raman spectra

Based on the previous Raman and IR spectroscopic studies on Pb-bearing chromate minerals (Frost 2004, Yang *et al.* 2007, Cooper *et al.* 2011, Kovrugin *et al.* 2018), we made the following tentative assignments of major Raman bands for evanichite: the relatively weak and broad bands centered at 3385 cm^{-1} can be ascribed to the O–H stretching vibrations in the OH groups. The
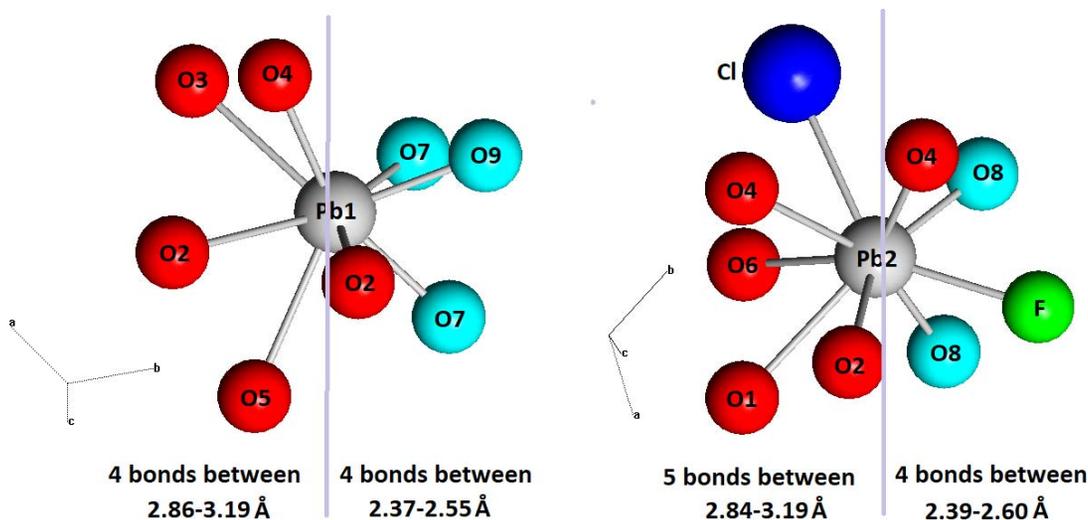

FIG. 4. The 8- and 9-coordinated Pb1 and Pb2 cations, respectively, in evanichite. Red, aqua, blue, and green spheres represent O, OH, Cl, and F atoms/groups, respectively. Both Pb1 and Pb2 have four short Pb-anion bonds on the right side separated by a vertical line.
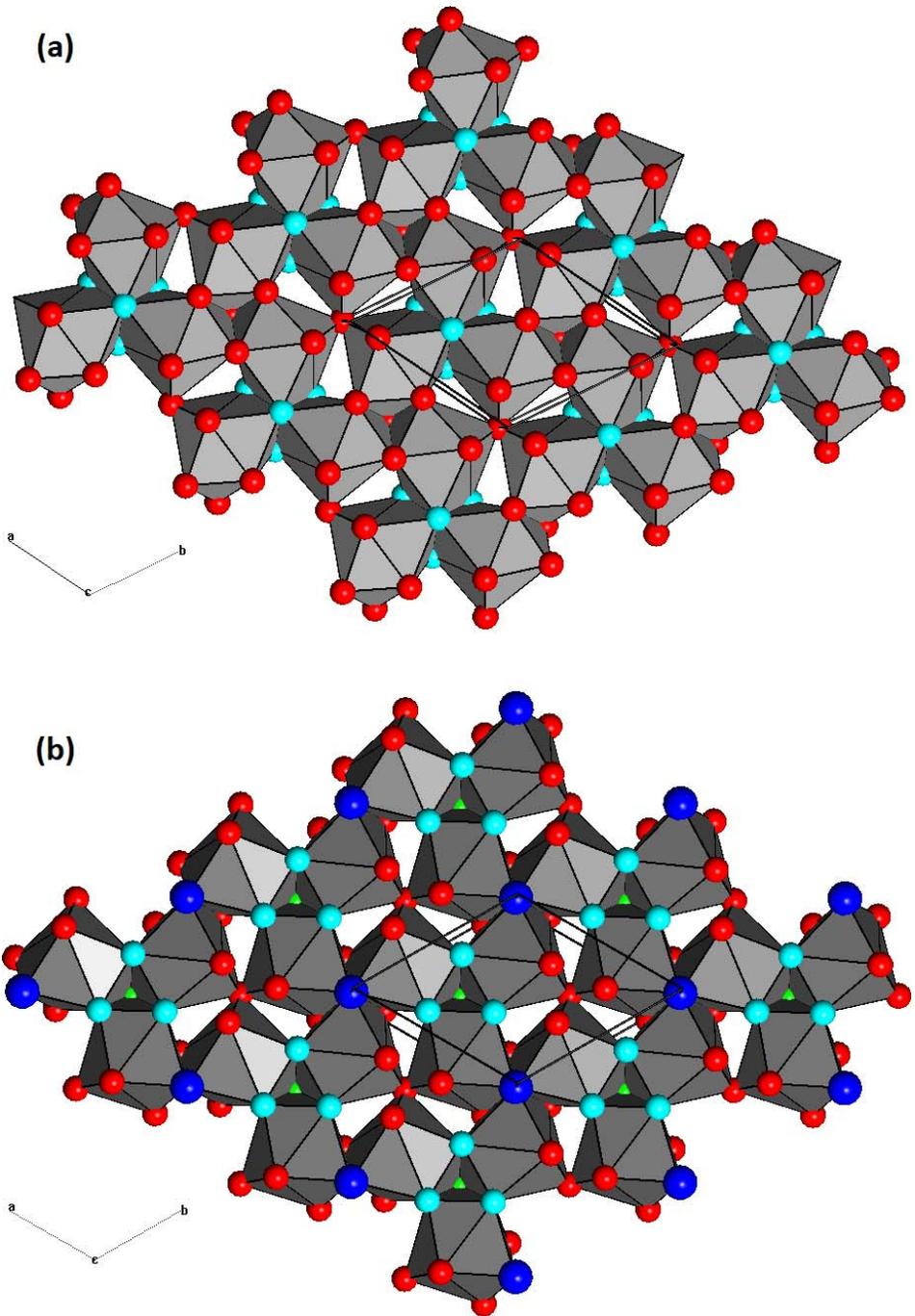
F𝗂𝗀. 5. Crystal structure of evanichite. (a) A layer of edge- and corner-shared, 8-coordinated Pb1 polyhedra and (b) a layer of edge- and corner-shared, 9-coordinated Pb2 polyhedra. Red, aqua, blue, and green spheres represent O, OH, Cl, and F atoms/groups, respectively.
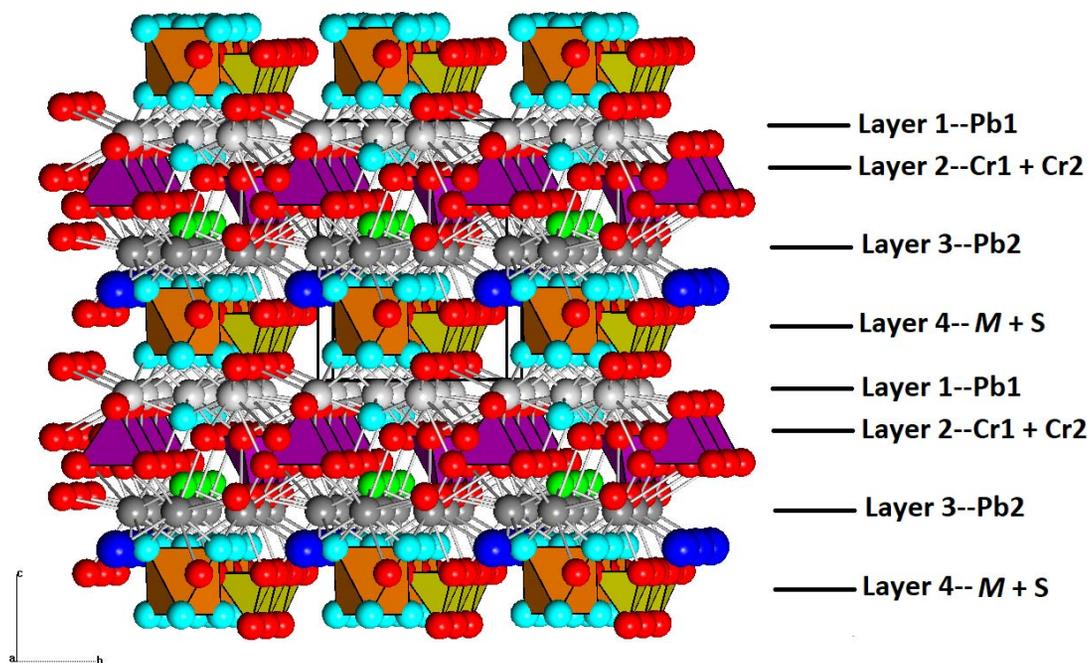
FIG. 6. Crystal structure of evanichite. The brown octahedra, purple tetrahedra, and yellow tetrahedra represent $Cr^{3+}(OH)_6$, $Cr^{6+}O_4$, and SO_4 groups, respectively. Gray, dark gray, blue, green, aqua, and red spheres represent Pb1, Pb2, Cl, F, OH, and O atoms/groups, respectively. For clarity, the Pb1 and Pb2 polyhedra are not drawn.

TABLE 7. BOND-VALENCE SUMS FOR EVANICHITE

Atom	Pb1	Pb2	M*	Cr1	Cr2	S	Sum
O1		0.138 ×3→		1.469			1.885
O2	0.359	0.088		1.373 ×3↓			1.875
	0.055						
O3	0.131 ×3→				1.532		1.925
O4	0.126	0.266			1.532 ×3↓		1.979
		0.055					
O5	0.110 ×3→					1.448	1.777
O6		0.136				1.458 ×3↓	1.627
O7	0.426		0.491 ×3↓				1.231
	0.314						
O8		0.468	0.481 ×2↓				1.272
		0.323					
O9	0.488 ×3→						1.456
F		0.264 ×3→					0.792
Cl		0.279 ×3→					0.838
Sum	2.009	2.019	2.915	5.589	6.127	5.928	

* The bond-valence sum for M was calculated based on $(0.88Cr^{3+} + 0.12Fe^{3+})$.
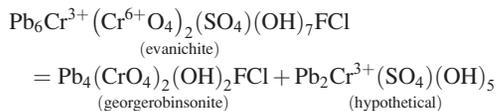
TABLE 8. LIST OF Pb CHROMATE MINERALS

Mineral	Formula	Ref.
Cassedanneite	$Pb_5(VO_4)_2(CrO_4)_2 \cdot H_2O$ unknown crystal structure	[1]
Chromschieffelinite	$Pb_{10}Te_6O_{20}(OH)_{14}(CrO_4) \cdot 5H_2O$	[2]
Crocoite	$Pb(CrO_4)$	[3, 4]
Embreyite	$Pb_2(Pb,Cu,\square)[(Cr,P)O_4]_2(H_2O,OH,\square)$	[5, 6, 22]
Fornacite	$Pb_2Cu(CrO_4)(AsO_4)(OH)$	[6–9]
Georgerobinsonite	$Pb_4(CrO_4)_2(OH)_2FCl$	[10]
Hemihedrite	$Pb_{10}Zn(CrO_4)_6(SiO_4)_2(OH)_2$	[8, 11, 12, 23]
Iranite	$Pb_{10}Cu(CrO_4)_6(SiO_4)_2(OH)_2$	[8, 13–15]
Macquartite	$Pb_7Cu_2(CrO_4)_4(SiO_4)_2(OH)_2$ no single-crystal X-ray data	[16, 17]
Phoenicochroite	$Pb_2O(CrO_4)$	[8, 18]
Reynoldsite	$Pb_2Mn_2O_5(CrO_4)$	[19]
Santanaite	$Pb^{2+}_9Pb^{4+}_2O_{12}(CrO_4)$ unknown crystal structure	[20]
Vauquelinite	$Pb_2Cu(CrO_4)(PO_4)(OH)$	[6, 8, 21]
Evanichite	$Pb_6Cr^{3+}(Cr^{6+}O_4)_2(SO_4)(OH)_7FCl$	This study

References: [1] – Cesbron et al. (1988); [2] – Kampf et al. (2012a); [3] – Quareni & de Pieri (1965); [4] – Effenberger & Pertlik (1986); [5] – Williams (1972); [6] – Khanin et al. (2015); [7] – Cocco et al. (1967); [8] – Cesbron & Williams (1980); [9] – Ksenofontov et al. (2014); [10] – Cooper et al. (2011); [11] – Williams & Anthony (1970); [12] – McLean & Anthony (1970); [13] – Bariand & Herpin (1963); [14] – Adib & Ottemann (1970); [15] – Yang et al. (2007); [16] – Williams & Duggan (1980); [17] – Cooper & Hawthorne (1994); [18] – Williams et al. (1970); [19] – Kampf et al. (2012b); [20] – Mücke (1972); [21] – Fanfani & Zanazzi (1968); [22] – Kovrugin et al. (2018); [23] – Lafuente et al. (2017).

bands between 800 and 1200 cm^{-1} are associated with the Cr^{6+}–O and S–O stretching modes within the SO_4 and CrO_4 tetrahedral groups, whereas the bands between 380 and 660 cm^{-1} are primarily attributable to the O–Cr^{6+}–O and O–S–O bending modes. The bands below 350 cm^{-1} are of a complex nature and are mostly associated with the rotational and translational modes of CrO_4 and SO_4 tetrahedra, (Cr^{3+},Fe^{3+})–O and Pb–O interactions. According to the correlation between O–H stretching frequencies (v_{O-H}) and O–H···O distances for minerals (Libowitzky 1999), the Raman band centered at 3385 cm^{-1} corresponds well with the O–O distances of 2.75–2.80 Å.

For comparison, the Raman spectra of Pb-bearing chromates vauquelinite, $Pb_2Cu(CrO_4)(PO_4)(OH)$ (http://rruff.info/R060926), and georgerobinsonite, $Pb_4(CrO_4)_2(OH)_2FCl$ (http://rruff.info/R110148), from the RRUFF Project were also plotted in Figure 3. The similarities among the three spectra are evident. The difference in peak intensities among the spectra principally results from the different crystal orientations when the data were collected, as well as from different mineral species. It is interesting to note that, although none of evanichite, georgerobinsonite, or vauquelinite contains H_2O in their ideal chemical formulae, all of their Raman spectra exhibit a weak band between 1640 and 1680 cm^{-1}, which is generally attributed to the H–O–H bending modes within H_2O groups. Perhaps, trace amounts of H_2O, more or less, indeed exist in these minerals.

Chemically, evanichite belongs to the group of Pb chromate minerals, which has 14 members (Table 8). In particular, the chemical composition of evanichite is most similar to that of georgerobinsonite, $Pb_4(CrO_4)_2$ $(OH)_2FCl$ (Cooper et al. 2011), which was also discovered from the Mammoth-St. Anthony mine, Tiger, Arizona, and has the same Pb:(XO_4) ratio of 2:1 as evanichite. In fact, the chemical formula of evanichite may be expressed as a combination of georgerobinsonite with a hypothetical compound:

$$\underset{\text{(evanichite)}}{Pb_6Cr^{3+}\left(Cr^{6+}O_4\right)_2(SO_4)(OH)_7FCl}$$
$$= \underset{\text{(georgerobinsonite)}}{Pb_4\left(CrO_4\right)_2(OH)_2FCl} + \underset{\text{(hypothetical)}}{Pb_2Cr^{3+}(SO_4)(OH)_5}$$

The $S^{6+} \leftrightarrow Cr^{6+}$ substitution in minerals and synthetic materials has been an interesting subject of both experimental and theoretical investigations because of its potential applications in removing toxic Cr^{6+} from environments polluted by steel production, leather tanning, corrosion, or mining processes (e.g., Fernández-González et al. 1999, Leisinger et al. 2010, 2012, Mireles et al. 2016 and references therein). Due to their similar crystal-chemical behaviors, S^{6+} and Cr^{6+} can readily substitute for each other to form complete solid solutions in numerous mineral systems, such as $BaCrO_4$ (hashemite) – $BaSO_4$ (baryte), $Pb_2O(CrO_4)$ (phoenicochroite) – $Pb_2O(SO_4)$ (lanarkite), $Pb_{10}Zn(CrO_4)_6(SiO_4)_2(OH)_2$ (hemihedrite) – $Pb_{10}Zn(SO_4)_6(SiO_4)_2(OH)_2$ (raygrantite), and Ca_6Al_2

$(SO_4)_3(OH)_{12} \cdot 27H_2O$ (ettringite) $-$ $Ca_6Al_2(CrO_4)_3$ $(OH)_{12} \cdot 26H_2O$ (siwaqaite). This may explain why there are chromate-phosphate, chromate-arsenate, chromate-vanadate, and chromate-silicate minerals (Table 8), but no chromate-sulfate mineral or synthetic compound had been reported until the discovery of evanichite. In this sense, not only does evanichite represent the first mineral that contains both Cr^{3+} and Cr^{6+}, but also the first chromate-sulfate compound with $(CrO_4)^{2-}$ and $(SO_4)^{2-}$ occupying distinct crystallographic sites. Hence, further investigations into the formation conditions of evanichite, such as pH, Eh, and temperature, will undoubtedly provide useful information on how to remove Cr^{6+} from polluted environments more efficiently and economically.

References Cited

Adib, D. & Ottemann, J. (1970) Some new lead oxide minerals and murdochite from T. Khuni Mine, Anarak, Iran. *Mineralium Deposita* **5**, 86–93.

Bariand, P. & Herpin, P. (1963) Une nouvelle espèce minérale: L'iranite, chromate hydraté de plomb. *Bulletin de la Societe Francaise Mineralogie et de Cristallographie* **86**, 113–135.

Bideaux, R.A. (1980) Famous mineral localities: Tiger, Arizona. *Mineralogical Record* **11**, 155–181.

Brese, N.E. & O'Keeffe, M. (1991) Bond-valence parameters for solids. *Acta Crystallographica* **B47**, 192–197.

Cesbron, F. & Williams, S.A. (1980) Iranitehémihédrite, bellite, phoenicochroite, vauquelinite et fornacite: synthèse et nouvelles données. *Bulletin de Minéralogie* **103**, 469–477.

Cesbron, F., Giraud, R., Pillard, F., & Poullen, J.-F. (1988) La cassedannéite, nouveau chromo-vanadate de plomb de Beresovsk (Oural). *Comptes Rendus de l'Académie des Sciences − Series II* **306**, 125–127.

Cocco, G., Fanfani, L., & Zanazzi, P.F. (1967) The crystal structure of fornacite. *Zeitschrift für Kristallographie* **124**, 385–397.

Cooper, M.A. & Hawthorne, F.C. (1994) The crystal structure of wherryite, $Pb_7Cu_2(SO_4)_4(SiO_4)_2(OH)_2$, a mixed sulfate-silicate with [[6] M(TO4)2φ] chains. *The Canadian Mineralogist* **32**, 373–380.

Cooper, M.A., Ball, N.A., Hawthorne, F.C., Paar, W.H., Roberts, A.C., & Moffatt, E. (2011) Georgerobinsonite, $Pb_4(CrO_4)_2(OH)_2FCl$, a new chromate mineral from the Mammoth - St. Anthony mine, Tiger, Pinal County,

Arizona: Description and crystal structure. *The Canadian Mineralogist* **49**, 865–876.

Downs, R.T., Bartelmehs, K.L., Gibbs, G.V., & Boisen, M.B., Jr (1993) Interactive software for calculating and displaying X-ray or neutron powder diffractometer patterns of crystalline materials. *American Mineralogist* **78**, 1104–1107.

Effenberger, H. & Pertlik, F. (1986) Four monazite type structures: Comparison of $SrCrO_4$, $SrSeO_4$, $PbCrO_4$ (crocoite), and $PbSeO_4$. *Zeitschrift für Kristallographie* **176**, 75–83.

Fanfani, L. & Zanazzi, P.F. (1968) The crystal structure of vauquelinite and the relationships to fornacite. *Zeitschrift für Kristallographie − Crystalline Materials* **126**, 433–443.

Fernández-González, A., Martín-Díaz, R., & Prieto, M. (1999) Crystallisation of $Ba(SO_4, CrO_4)$ solid solutions from aqueous solutions. *Journal of Crystal Growth* **200**, 227–235.

Frost, R.L. (2004) Raman microscopy of selected chromate minerals. *Journal of Raman Spectroscopy* **35**, 153–158.

Kampf, A.R., Mills, S.J., Housley, R.M., Rumsey, M.S., & Spratt, J. (2012a) Lead-telluriumoxysalts from Otto Mountain near Baker, California: VII. Chromschieffelinite, $Pb_{10}Te_6O_{20}(OH)_{14}(CrO_4)(H_2O)_5$, the chromate analog of schieffelinite. *American Mineralogist* **97**, 212–219.

Kampf, A.R., Mills, S.J., Housley, R.M., Bottrill, R.S., & Kolitsch, U. (2012b) Reynoldsite, $Pb_2Mn^{4+}_2O_5(CrO_4)$, a new phyllomanganate-chromate from the Blue Bell claims, California and the Red Lead mine, Tasmania. *American Mineralogist* **97**, 1187–1192.

Khanin, D.A., Pekov, I.V., Pakunova, A.V., Ekimenkova, I.A., & Yapaskurt, V.O. (2015) Natural system of fornacite–vauquelinite–embreyite solid solutions and variations in the chemical composition of these minerals from occurrences of the Urals. *Zapiski Rossiiskogo Mineralogicheskogo Obshchestva* **144**, 36–60 (in Russian).

Kovrugin, V.M., Siidra, O.I., Pekov, I.V., Chukanov, N.V., Khanin, D.A., & Agakhanov, A.A. (2018) Embreyite: Structure determination, chemical formula and comparative crystal chemistry. *Mineralogical Magazine* **82**, 275–290.

Ksenofontov, D.A., Kabalov, Y.K., Pekov, I.V., Zubkova, N.V., Ekimenkova, I.A., & Pushcharovskii, D.Y. (2014) Refinement of the crystal structure of fornacite using the Rietveld method. *Doklady Earth Sciences* **456**, 520–523.

Lafuente, B., Downs, R.T., Origlieri, M.J., Domanik, K.J., Gibbs, R.B., & Rumsey, M.S. (2017) New data on hemihedrite from Arizona. *Mineralogical Magazine* **81**, 1021–1030.

Leisinger, S.M., Lothenbach, B., Le Saout, G., Kägi, R., Wehrli, B., & Johnson, C.A. (2010) Solid solutions

between CrO_4- and SO_4-ettringite $Ca_6(Al(OH)_6)_2$ $[(CrO_4)_x(SO_4)_{1-x}]_3 \cdot 26H_2O$. *Environmental Sciences and Technology* **44**, 8983–8988.

LEISINGER, S.M., LOTHENBACH, B., LE SAOUT, G., & JOHNSON, C.A. (2012) Thermodynamic modeling of solid solutions between monosulfate and monochromate $3CaO \cdot Al_2O_3 \cdot Ca[(CrO_4)_x(SO_4)_{1-x}] \cdot nH_2O$. *Cement and Concrete Research* **42**, 158–165.

LIBOWITZKY, E. (1999) Correlation of O–H stretching frequencies and O–H···O hydrogen bond lengths in minerals. *Monatshefte für Chemie* **130**, 1047–1059.

MANDARINO, J.A. (1981) The Gladstone-Dale relationship: Part IV. The compatibility concept and its application. *The Canadian Mineralogist* **19**, 441–450.

MCLEAN, W.J. & ANTHONY, J.W. (1970) The crystal structure of hemihedrite. *American Mineralogist* **55**, 1103–1114.

MIRELES, I., REYES, I.A., FLORES, V.H., PATIÑO, F., FLORES, M.U., REYES, M., ACOSTA, M., CRUZ, R., & GUTIÉRREZ, E.J. (2016) Kinetic analysis of the decomposition of the $KFe_3(SO_4)_{2-x}(CrO_4)_x(OH)_6$ jarosite solid solution in $Ca(OH)_2$ medium. *Journal of Brazilian Chemistry Society* **27**, 1014–1025.

MÜCKE, A. (1972) Santanait, ein neues Bleichromat-Mineral. *Neues Jahrbuch für Mineralogie, Monatshefte* **10**, 455–458.

O'NEILL, H.S.C. & DOLLASE, W.A. (1994) Crystal structures and cation distributions in simple spinels from Powder XRD structural refinements: $MgCr_2O_4$, $ZnCr_2O_4$, Fe_3O_4 and the temperature dependence of the cation distribution in $ZnAl_2O_4$. *Physics and Chemistry of Minerals* **20**, 541–555.

ORIGLIERI, M.J., DOWNS, R.T., THOMPSON, R.M., POMMIER, C.J.S., DENTON, M.B., & HARLOW, G.E. (2003) High-pressure crystal structure of kosmochlor, $NaCrSi_2O_6$, and systematics of anisotropic compression in pyroxenes. *American Mineralogist* **88**, 1025–1032.

PANCZNER, W.D. (1982) The Mammoth-St. Anthony Mine Tiger, Arizona. *Rocks & Minerals* **57**, 5–10.

QUARENI, S. & DE PIERI, R. (1965) A three-dimensional refinement of the structure of crocoite, $PbCrO_4$. *Acta Crystallographica* **19**, 287–289.

ROBINSON, K., GIBBS, G.V., & RIBBE, P.H. (1971) Quadratic elongation: A quantitative measure of distortion in coordination polyhedra. *Science* **172**, 567–570.

SHELDRICK, G.M. (2015a) SHELXT – Integrated space-group and crystal structure determination. *Acta Crystallographica* **A71**, 3–8.

SHELDRICK, G.M. (2015b) Crystal structure refinement with SHELX. *Acta Crystallographica* **C71**, 3–8.

SHIMONI-LIVNY, L., GLUSKER, J.P., & BOCK, C.W. (1998) Lone pair functionality in divalent lead compounds. *Inorganic Chemistry* **37**, 1853–1867.

WILLIAMS, S.A. (1972) Embreyite, a new mineral from Berezov, Siberia. *Mineralogical Magazine* **38**, 790–793.

WILLIAMS, S.A. & ANTHONY, J.W. (1970) Hemihedrite, a new mineral from Arizona. *American Mineralogist* **55**, 1088–1102.

WILLIAMS, S.A. & DUGGAN, M. (1980) La macquartite: Un nouveau silico-chromate de Tiger, Arizona. *Bulletin de Minéralogie* **103**, 530–532.

WILLIAMS, S.A., MCLEAN, W.J., & ANTHONY, J.W. (1970) A study of phoenicochroite – Its structure and properties. *American Mineralogist* **55**, 784–792.

YANG, H., SANO, J.L., EICHLER, C., DOWNS, R.T., & COSTIN, G. (2007) Iranite, $CuPb_{10}(CrO_4)_6(SiO_4)_2(OH)_2$, isomorphous with hemihedrite. *Acta Crystallographica* **C63**, i122–i124.